KfK 3097 B
Dezember 1980

Neutron and Charged Particle Production Yields and Spectra from Thick Metal Targets by 590 MeV Protons

S. Cierjacks, M. T. Rainbow, M. T. Swinhoe, L. Buth
Institut für Kernphysik

Kernforschungszentrum Karlsruhe

KERNFORSCHUNGSZENTRUM KARLSRUHE
Institut für Kernphysik

KfK 3097 B

Neutron and Charged Particle Production Yields and Spectra from Thick Metal Targets by 590 MeV Protons*

S. Cierjacks, M.T. Rainbow, M.T. Swinhoe and L. Buth

* presented at the ICANS-IV Meeting 1980,
KEK National Laboratory for High-Energy Physics,
Tsukuba, Japan

Kernforschungszentrum Karlsruhe GmbH, Karlsruhe

Kernforschungszentrum Karlsruhe GmbH
ISSN 0303-4003

Abstract

Time-of-flight measurements of neutrons and protons produced by bombardment of thick lead, lead-bismuth and uranium targets with 590 MeV protons have been carried out at the SIN cyclotron. Measurements were made at angles of 30^{o}, 90^{o} and 150^{o} for different penetration depths of protons in a 10 cm diam x 60 cm long target. The detector was an NE 213 liquid scintillator. Differential neutron data are presented and compared with intranuclear-cascade-evaporation model calculations. First results of the secondary proton yield are also presented. The neutron yield and spectrum produced from a moderator around the target was determined from 5 - 140 MeV using an unfolding method.

Ausbeuten und Spektren schneller Neutronen und Protonen aus dem Beschuß von dicken Metalltargets mit 590 MeV Protonen

Zusammenfassung

Mit Hilfe der Flugzeitmethode wurden am SIN absolute Ausbeuten und Spektren schneller Neutronen und Protonen gemessen, die bei Beschuß von dicken Blei-, Blei-Wismut- bzw. Urantargets mit 590 MeV Protonen entstehen. Ausbeuten und Spektren wurden getrennt für die drei Emissionswinkel 30^{o}, 90^{o} und 150^{o} sowie für verschiedene Eindringtiefen der Protonen in 60 cm lange Schwermetalltargets von 10 cm Durchmesser aufgenommen. Zum Nachweis der Sekundärteilchen wurde ein NE 213 Flüssigkeitsszintillator verwendet. Im Bericht werden differentielle Neutronendaten gezeigt und mit Vorhersagen des intranuklearen Kaskaden-Verdampfungsmodells verglichen. Erste Ergebnisse von Ausbeuten und Spektren sekundärer Protonen werden ebenfalls gezeigt. Weiterhin wurden die Spektren schneller Neutronen mit Energien zwischen 5 und 140 MeV gemessen, die in einem das Schwermetall umgebenden Moderator entstehen. Die Berechnung solcher Spektren erforderte eine besondere Entfaltungsmethode.

NEUTRON AND CHARGED PARTICLE PRODUCTION YIELDS AND SPECTRA FROM THICK METAL TARGETS BY 590 MEV PROTONS

1. INTRODUCTION

The present experiments were performed as part of the feasibility study for a new German spallation source. Concerning neutronic aspects of such a source an accurate knowledge of depth and angular dependent yields and spectra from the bare target is important, since these determine all subsequent processes in the moderator-reflector system. In the past, several measurements have been made to determine the total neutron yields as a function of both projectile energies and target materials. However, in most of these only the number of moderated neutrons per incident proton were observed. This number is, in general, different and smaller than the total number of neutrons emitted from the bare target due to the fraction of fast neutrons which are not counted by the thermal neutron detectors employed. Only a few measurements of fast neutron yields and spectra have been made so far. Comparisons of these with theoretical model calculations have often revealed significant discrepancies. This applies, in particular, to the high energy tails of the angular dependent spectra. In view of this fact, the experimental results presently

provide the best data base for feasibility studies of advanced spallation neutron sources. These results can also be used to improve existing computer codes which predict neutron yields and spectra.

Another important piece of information needed to judge the usefulness of a spallation facility as a source of thermal neutrons concerns the background of fast neutrons escaping together with the thermal beam through the beam tubes. These fast neutrons could create shielding problems and might be a source of unwanted background in certain experiments. Therfore, our experimental program included also a study of this quantity. First results of this kind gave information on the fast neutron background associated with a light water moderated neutron beam from Pb-Bi and U spallation targets.

In section 2 of this paper the experimental set up and electronics are described. Section 3 gives a brief summary of the method of data analysis. Typical results of neutron spectra from the bare target are presented in section 4 and are compared to theoretical calculations. Section 5 describes a first investigation of the spectrum from the moderated source and section 6 summarizes the current state of the experimental program.

2. EXPERIMENTAL DETAILS

The measurements were performed at the Swiss Institute for Nuclear Research (SIN) using the 590 MeV proton beam from the ring cyclotron. A schematic diagram of the experimental arrangement is presented in Figure 1. The proton beam, which was pulsed at 16.9 MHz with a 0.2 ns pulse width, was focussed to 2 cm diameter onto a cylindrical lead target. The target was composed of twelve cylindrical blocks, each 5 cm long and 10 cm in diameter, to give an overall length of 60 cm.

Measurements of secondary particle emission from the target were made at 30°, 90° and 150° via an iron collimator which was $\sim$ 1 m thick. Measurements of particle emission corresponding to different distances into the target were made by moving the target along the beam axis so that individual blocks were opposite the collimator entrance.

The principal detector used was a 3.0 cm thick, 4.5 cm diameter NE 213 liquid scintillator; used for its pulse shape (particle) discrimination properties. A 0.5 cm thick plastic scintillator was located immediately in front of the liquid scintillator to provide further assistance with particle identification. The passage of charged particles causes both detectors to generate signals, whereas neutral particles, in general, give a pulse in only one. Charged particle spectra (for protons) were accumulated by operating the two detectors in coincidence. Neutral particle spectra (for neutrons) were accumulated by operating the plastic scintillator as a veto detector. Background measurements were performed with the target block opposite the collimator entrance removed.

A block diagram of the electronics is presented in Figure 2. The pulse height signals from the liquid scintillator were fed through two amplifier channels, one with ten times the gain of the other, to cover the required dynamic range. The timing signal from the liquid scintillator was involved in three functions:

(i) In conjunction with the timing signal from the plastic scintillator, it was used to operate a coincidence unit, in coincidence or veto mode, to generate a master trigger signal which notified the computer that an event of interest had occurred and the gates to the ADCs should be opened.

(ii) It was analysed by a pulse shape discrimination unit. The result of this analysis appeared as a 'pulse shape discrimination time' signal from the TAC, the output of which went to ADC3.

(iii) It started the TAC which provided time-of-flight information via ADC4. This TAC was stopped by a timing signal derived from the cyclotron high frequency.

The contents of the four ADCs were stored event by event on magnetic tape to allow subsequent 2-parameter particle discrimination and time-of-flight analysis.

The charge deposited in the target was monitored by recording the output of the proton beam monitor (see Figure 1). This system consists of a carbon scatterer located in the beam and a pair of plastic scintillators which operated in coincidence to detect scattered protons. It was calibrated by determining the ratio of the count rate of the monitor to that of another plastic scintillator placed in the direct proton beam at reduced current.

The number of master triggers applied to the computer was recorded and used, in conjunction with the number of accepted events, to evaluate the dead time correction.

3. DATA ANALYSIS

The analysis of the neutron data (neutral particle spectra) began with the separation of events into neutron and non-neutron (gamma) by a consideration of pulse height versus 'pulse shape discrimination time'. The neutron events from the corresponding background run were then subtracted. The data were subsequently sorted into suitable time-of-flight bins. The corresponding neutron energies were calculated relativistically according to the time of occurence of the γ-flash and the flight path length.

The beam pulse frequency (16.9 MHz) and flight path lengths (e.g. 1.17 m at 90°) resulted in the production of a single overlap in part of each time-of-flight spectrum. For example, 1.74 MeV neutrons appear to have the same flight time as 500 MeV neutrons for measurements at the 90° position. Separation of the response due to high energy neutrons from that due to low energy neutrons, was achieved by linear extrapolation of the high energy pulse height response down to the bias level. The error associated with this procedure is small due to the shape of the distributions.

The contents of each time-of-flight bin were integrated and the results divided by the detection efficiency of the NE 213 liquid scintillator. The Monte Carlo code of Cecil et al. [1] was used to calculate the required efficiency. The shape of the pulse height spectra produced by the code are in good agreement with the measured spectra in individual time bins. This is the case even when the ranges of the charged particles produced in the detector are greater than the detector dimensions. This gives some confidence in the operation of the code. The bias level used in the calculations was determined by locating the upper edges of the pulse height spectra in various time-of-flight bins and extrapolating to find the proton energy corresponding to the pulse height threshold.

It is our intention to experimentally determine the efficiency of the detectors at high energy where the code is least reliable. A preliminary determination of the efficiency at 350 MeV suggests the code may overpredict the efficiency in this region.

The data were finally scaled by the solid angle subtended by the detector, the dead-time correction factor and the number of incident protons to produce the absolute neutron yield as neutrons per steradian per MeV per proton incident on the target per 5 cm of target length. Finally the results for various distances into the target were added to produce the absolute neutron yield from the whole target.

The analysis of the proton data (charged particle spectra) is much simpler. The response of the liquid scintillator to protons of a particular energy appears as a Gaussian peak in the pulse height spectrum. The data were sorted into time bins as for the neutron case. The peaks in the pulse height spectra

in the various time-of-flight bins were located and the area under the peaks above the background was evaluated. The measured spectrum only extends down to 27 MeV due to absorption in the plastic scintillator, which stops protons of lower energy. The absolute secondary proton yield was evaluated in the same manner as the neutron yield.

A correction was made to both the neutron and proton spectra for the measured time resolution of the system. This was done by the second derivative method [2] .

4. RESULTS

Figure 3 shows the spectrum of neutrons emitted from the first lead block in the target (0 to 5 cm) at 90^{o} to the incident proton beam. This is compared to the results of measurements made at Los Alamos [3] at an angle of 112^{o} for 800 MeV protons incident on a thin (0.45 cm) lead target. The Los Alamos spectrum has been normalized to give an integral number of neutrons per incident proton (n/p) which is consistent with the data of Fraser et al. [4]. Despite the fact that the two spectra are not directly comparable there is an obvious similarity in shape.

The angular dependence of the neutron spectra from the first block is shown in Figure 4, for angles of 30, 90 and 150^{o} with respect to the incident beam. These exhibit the well known two-component shape originating from contributions of evaporation processes and direct cascade reactions (the latter of which produces the broad shoulder around 50 MeV). As expected the high energy component is most pronounced at 30^{o}, while its contribution to the 150^{o} spectrum is small. The yield of low energy neutrons ($E_n < 10$ MeV)

appears to be the same at 150° and 90° but at 30° is reduced, probably due to the greater amount of lead that the neutrons must penetrate. (For blocks other than the first it is to be expected that the low energy yields would be the same for 30° and 150° but greater for 90° due to the differences of path length through the lead.)

The neutron yield above 1.5 MeV is shown in Figure 5 as a function of distance into the target. These results show that the yield from distances greater than 30 cm is less than 1 per cent of the total yield. The experimental results suggest that the neutron yield decreases monotonically through the target. However, there is calculational evidence which indicates that the yield actually peaks at small distance from the front surface. This feature is indicated by the solid line drawn through the experimental results.

The sum of the 90° differential spectra for the whole target is presented in Figure 6. It is a reasonable approximation to take this spectrum as representing the average spectrum for all angles of emission with respect to the incident proton beam. On this basis 12.2 neutrons with a mean energy of 22.2 MeV are emitted from the whole target into all angles per incident proton.

The target integrated 90° spectrum from Figure 5 is compared to a recent calculation performed at KFA, Jülich [5] in Figure 7. The calculational method is based on the 3-dimensional 'High Energy Nucleon-Meson Transport Code, HETC' [6] . The results presented are from a preliminary calculation of the energy spectrum of neutrons emitted from the whole target (15 cm diam., 80 cm long) at all angles. Also included for comparison are the

Los Alamos experimental results [3] already presented in Figure 3 and some calculational results from the same laboratory reported by Fullwood et al. [7] . This latter calculation gives the neutron emission from a lead target (15 cm diam., 30 cm long) for an incident proton energy of 800 MeV. The spectra are presented on a relative lethargy scale so that the fraction of neutrons below or above a certain energy is represented by areas under the curves. They have been normalized to the respective n/p values [4] . It is clear, despite the fact that the spectra are not directly comparable, that at the present time calculations are producing spectra which are much softer than those measured.

The differential spectrum of secondary protons emitted from the first block (0 to 5 cm) in the target at 90° is shown in Figure 8. This result shows that the contribution from elastic scattering in lead is small. The bulk of the spectrum is the result of inelastic and nuclear reactions. From our experimental data we have made an estimate of the secondary proton yield. Our preliminary value is 0.11 secondary protons per incident proton.

5. MEASUREMENTS OF THE HIGH ENERGY COMPONENT OF THE NEUTRON SPECTRUM FROM A MODERATED SOURCE

The neutron spectrum from a moderated source covers the energy range from thermal to hundreds of MeV. The range of interest for these measurements of the "high energy" part of the spectrum includes all those neutrons above a few MeV. Even though time-of-flight measurements of fast neutron spectra would have been most desirable, this method was not applicable at the SIN cyclotron,

where the only available pulse structure comes from the cyclotron microstructure. This time structure is much too narrow compared with the large time spread associated with the moderation process and so an unfolding method was necessary.

The moderated source was a 15 cm diameter heavy metal target (lead or uranium) in a cubic tank (of side 2 m) of light water. The geometry of the experiment is shown in Figure 9. The detector, an 8.9 cm thick NE 213 scintillator, was placed approximately 8 m from the target at 30° to the incident beam direction. The collimator defined a region above the bare target so that neutrons directly from the target could not be seen. The same electronics and data recording system were used as for the bare target measurements described above, with the omission of the time-of-flight parameter.

The results for targets of lead and uranium are shown in Figure 10. These were obtained by rectangularly unfolding the pulse height distributions of the detector, and are absolutely normalized to 10 mA proton current at a distance of 6 m from the target.

By simulating the experiment using detector response functions generated by the Monte-Carlo program of Cecil et al. [1], the error involved in the analysis was estimated. It appears that the rectangular unfolding gives a good estimate of the total number of neutrons, but underestimates the fraction of neutrons at high energies. The latter is to be expected as the response of the scintillator to monoenergetic neutrons above $\sim$ 30 MeV is far from rectangular due to charged particles

produced in neutron interactions with carbon, and, in addition, the loss of energetic charged particles from the detector.

In order to achieve more reliable results for the high energy tails of the spectra, work is in progress on an iterative method of unfolding. Combined with the use of a thicker detector (30 cm NE 213) this should allow reasonable spectra determination up to 200 MeV. The poorer energy resolution resulting from the larger detector size does not appear to be an important disadvantage for the intended application which deals with relatively smooth neutron spectra.

6. PROSPECTS

Experimental measurements have been made of the absolute yield, angular distribution and spectra for neutrons and protons produced by the bombardment of both lead and uranium thick targets with 590 MeV protons from the SIN cyclotron. Work is still in progress on the analysis of these data. Before the end of the year it is planned to carry out similar measurements at the higher proton energy of 1.1 GeV using the SATURNE accelerator in France. At this machine additional spectra measurements of fast neutrons from a moderated source are also planned, evaluating, in particular, the differences for "wing" and "slab" geometry for the moderator. Information relevant to the theoretical models involved in the computer codes can best be obtained from measurements on thin targets, and an experiment of this type has also been scheduled.

ACKNOWLEDGEMENTS

The authors are indebted to Dr. W. Kluge and his group members, in particular DP U. Klein and Dr. H. Matthäy, for providing invaluable support during the initial phase of the experimental programme. The help of the SIN staff, especially Dr. W. Fischer and Dr. C. Tschalär, is also gratefully acknowledged.

REFERENCES

1. R.A. Cecil, B.D. Anderson and R. Madey, Nucl. Instrum. Methods 161, 439 (1979)

2. H.W. Schmitt, W.E. Kiker and C.W. Williams, Phys. Rev. B 137, 837 (1965)

3. S.D. Howe, N.S.P. King, P.W. Lisowski and G.J. Russell, Contr. Int. Conf. on Nuclear Cross Sections for Technology, Knoxville, Oct. 1979

4. J.S. Fraser, R.E. Green, J.W. Hilborn, J.C.D. Milton, W.A. Gibson, E.E. Gross and A. Zucker, Phys. Canada 21 (2), 17 (1965); G.A. Bartholomew and P.R. Tunicliffe (Eds.) AECL-2600 (Chalk River) (1966) p. VII, 12

5. D. Filges, P. Cloth, R.D. Neef and G. Sterzenbach, Contr. to Spallation Source Meeting, Bad Königstein, 18-20 March, 1980

6. HETC - ORNL-4744 (Oak Ridge National Laboratory)

7. R.R. Fullwood, J.D. Cramer, R.A. Haarman, R.P. Forrest, Tr. and R.G. Schrandt, LA-4789 (Los Alamos Scientific Laboratory) (1972)

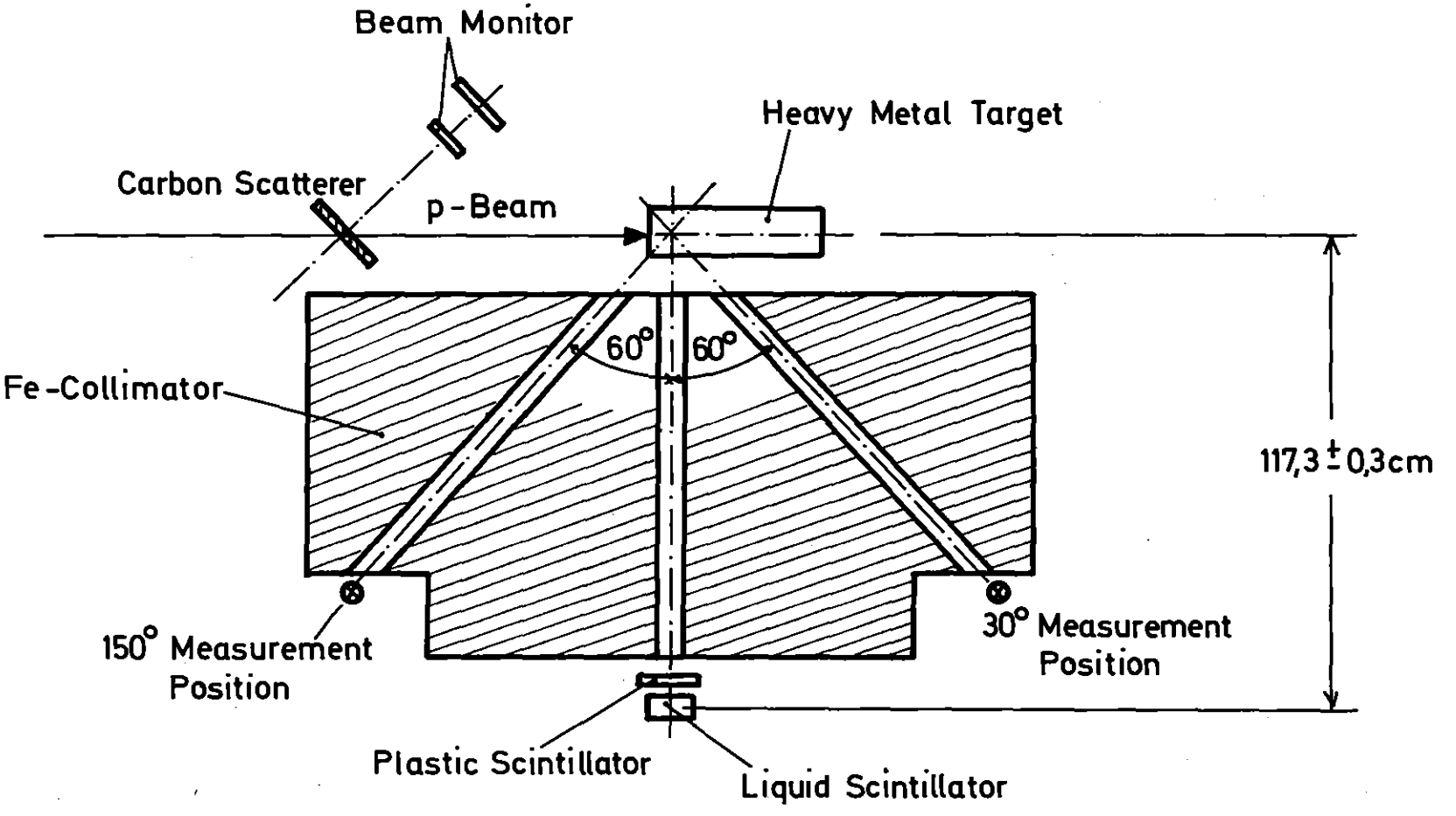

Figure 1 - Schematic diagram of the experimental arrangement for the SIN time-of flight experiments

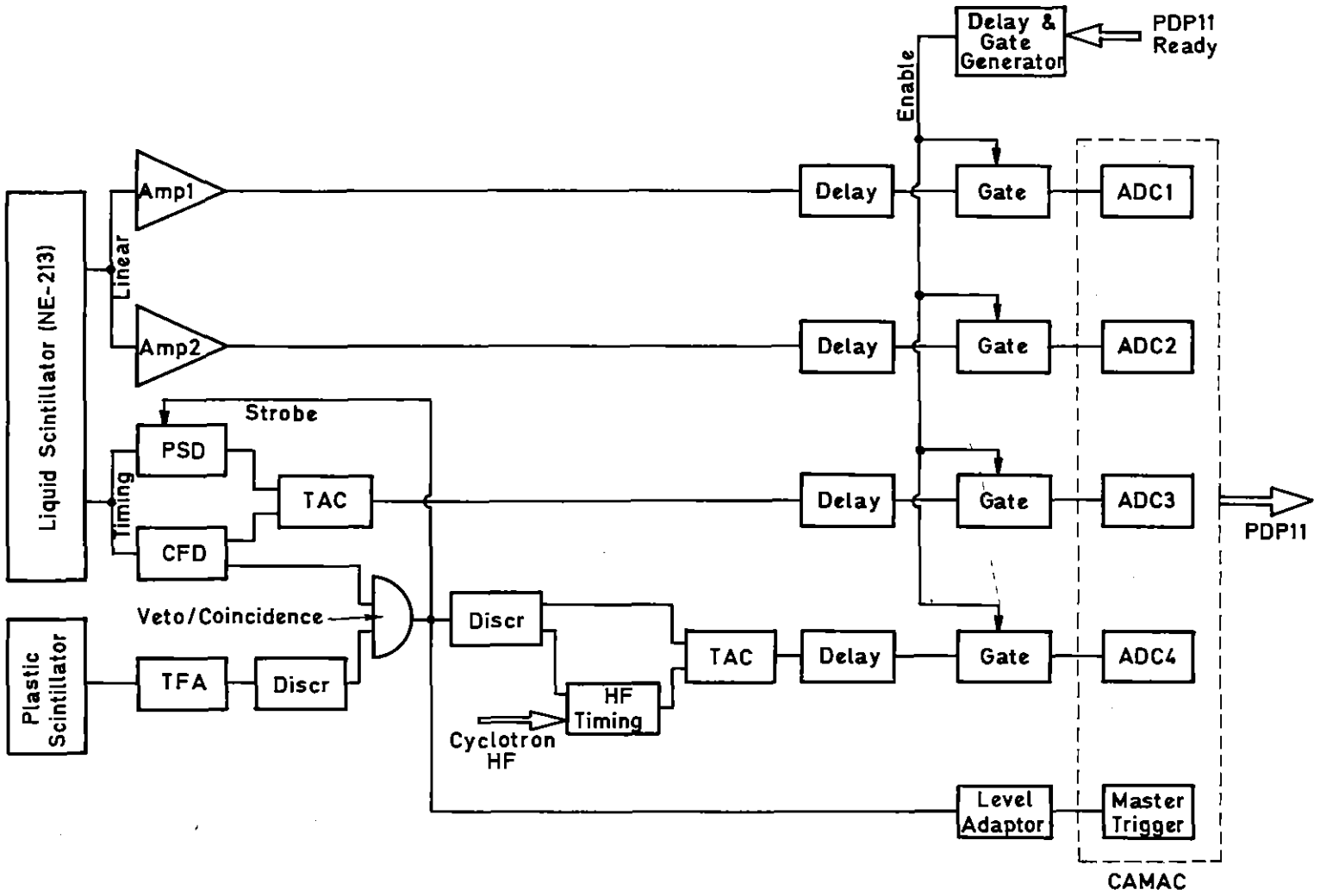

Figure 2 - Block diagram of the electronic system for the SIN time-of-flight experiments

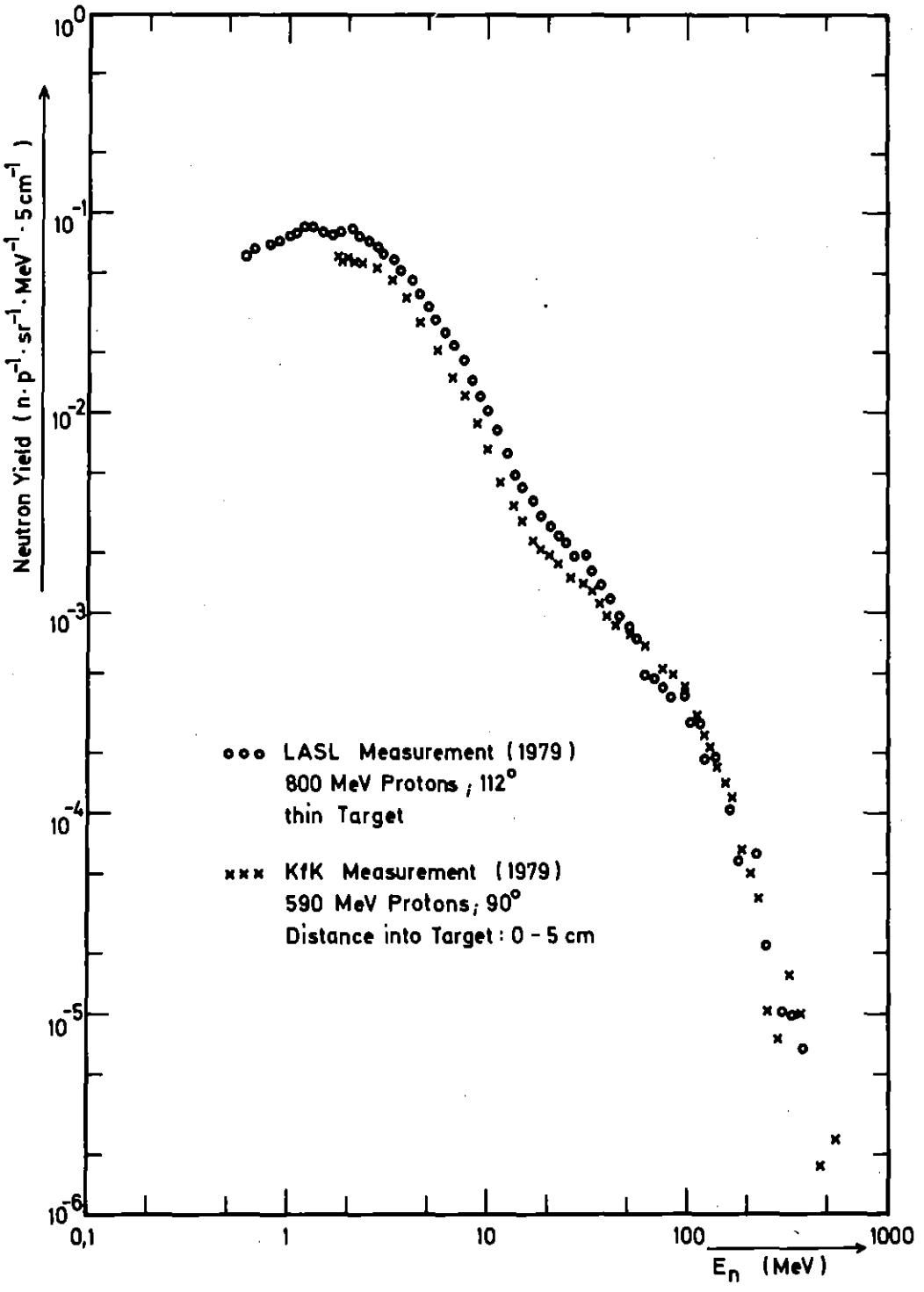

Figure 3 - Differential spectrum of neutrons emitted at 90° from the first 5 cm of the 10 cm diam. lead target for an incident proton energy of 590 MeV. The LASL spectrum was obtained at 112° for 800 MeV protons incident upon a thin lead target

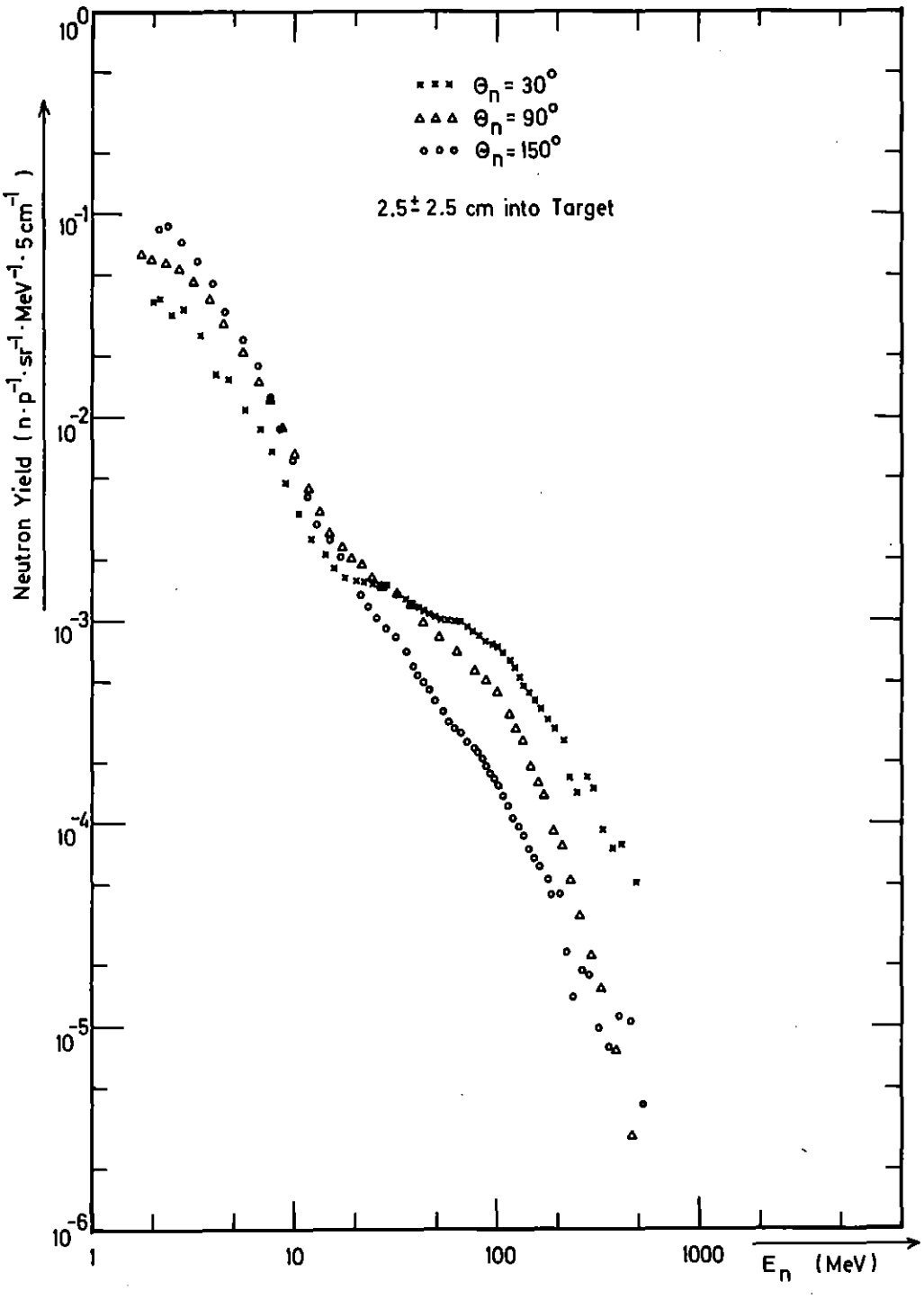

Figure 4 - Differential spectra of neutrons at 30°, 90° and 150° from the first 5 cm of the 10 cm diam. lead target for an incident proton energy of 590 MeV

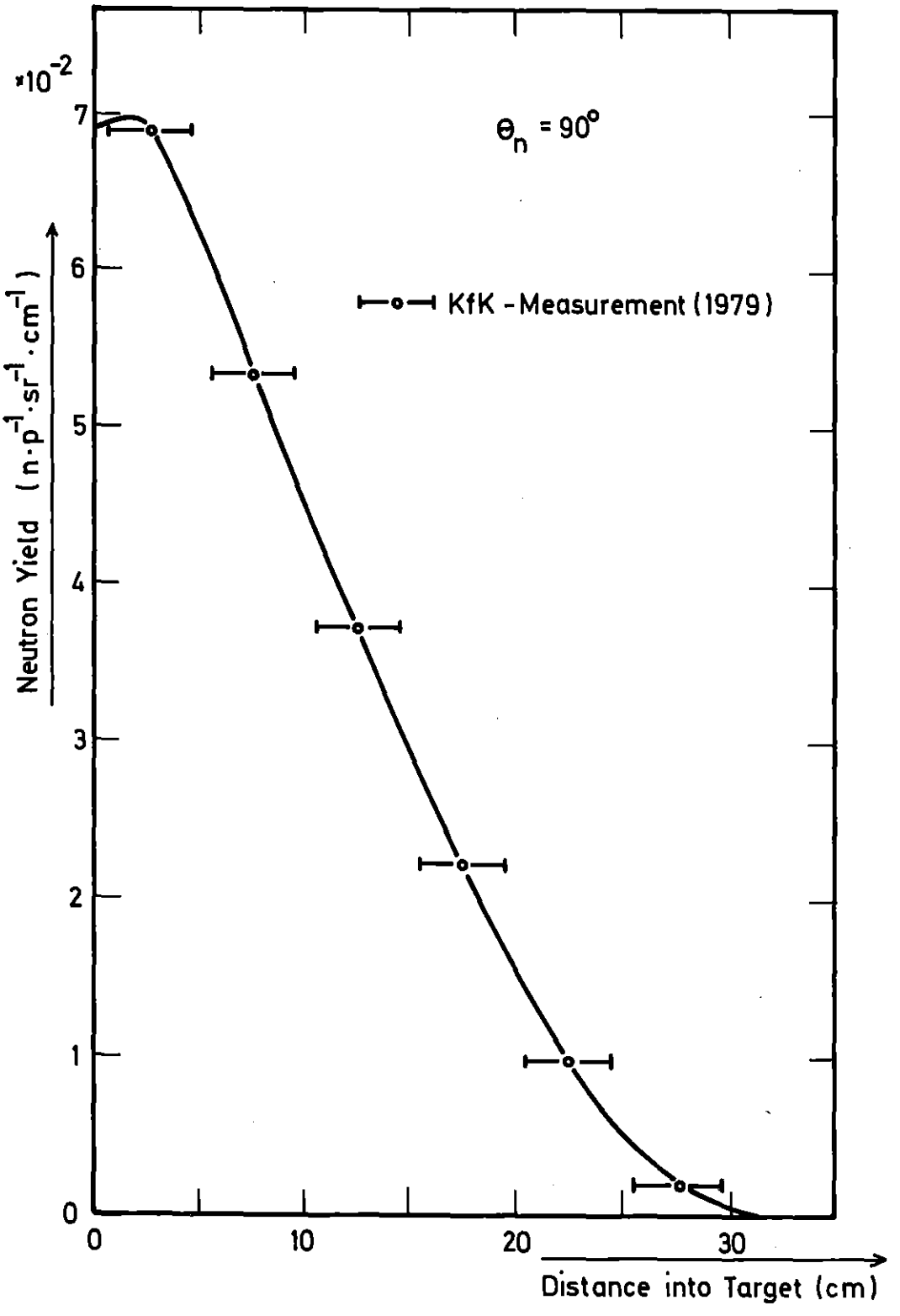

Figure 5 - Total neutron yield at 90° (E_n > 1.5 MeV) as a function of proton penetration into the 10 cm diam. lead target

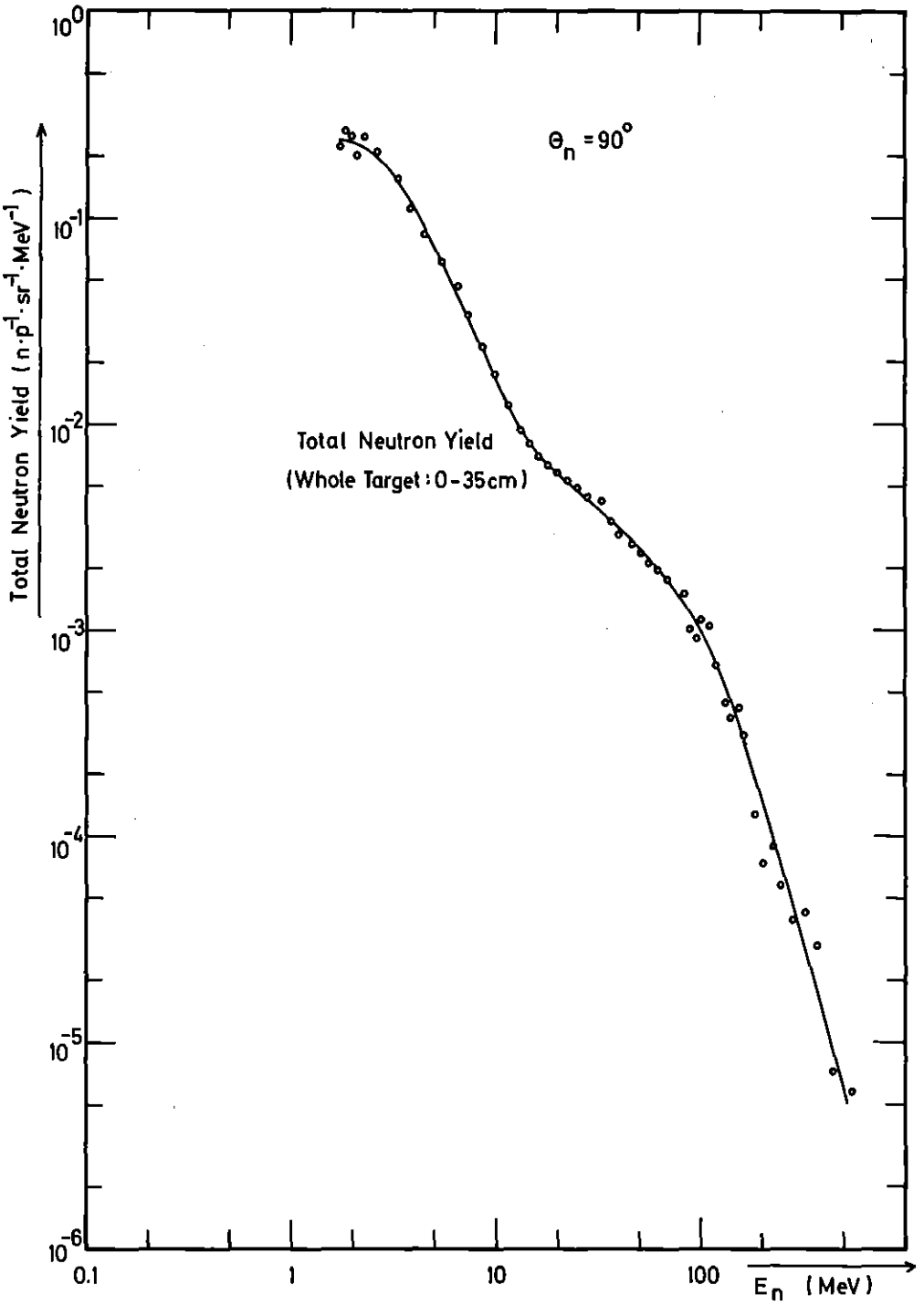

Figure 6 - Spectrum of neutrons emitted at 90° integrated over the first 35 cm of a thick lead target

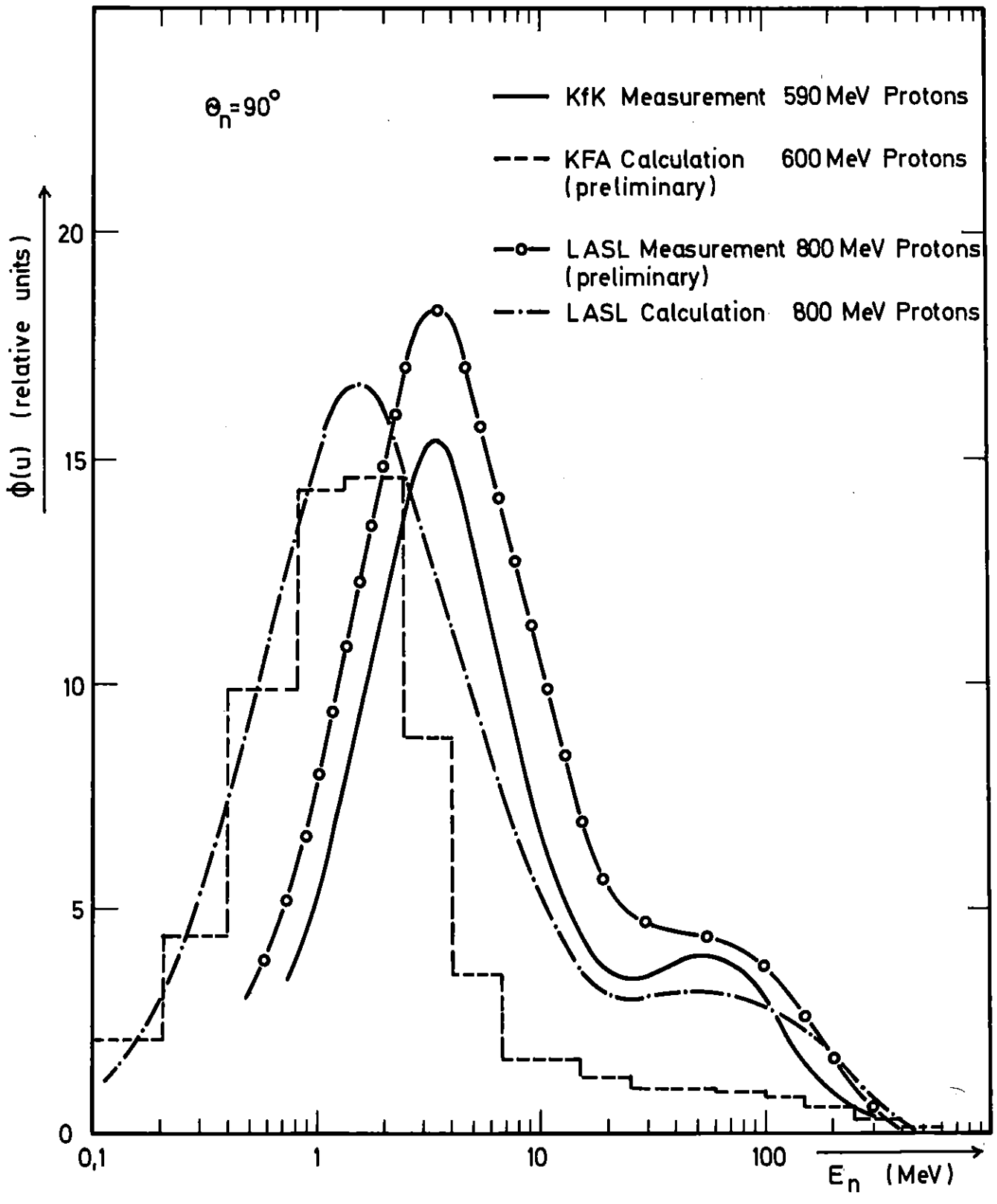

Figure 7 - Measured and calculated neutron spectra for lead targets normalized to respective n/p values (see text)

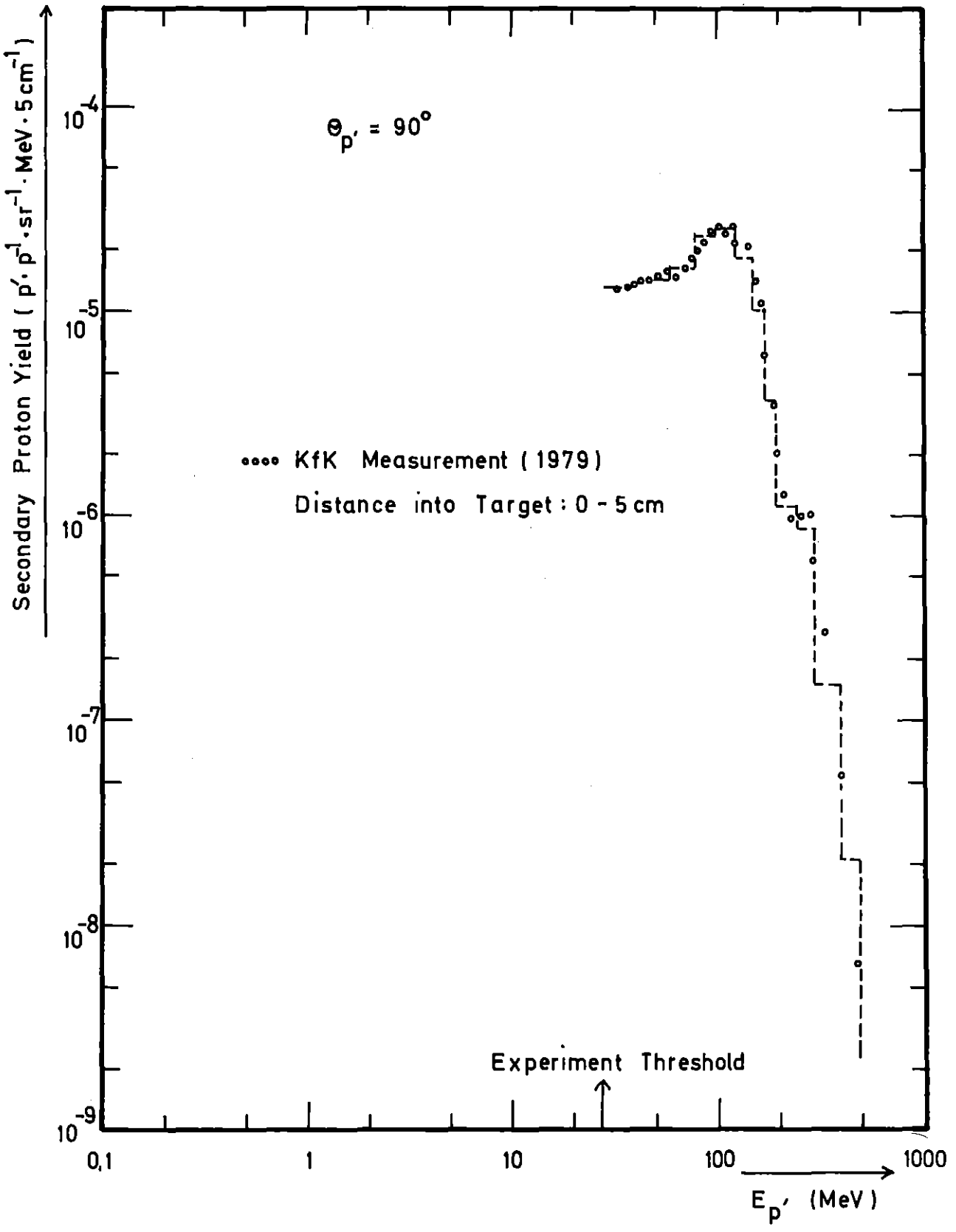

Figure 8 - Differential spectrum of secondary protons emitted at 90° from the first 5 cm of the 10 cm diam. lead target for an incident proton energy of 590 MeV

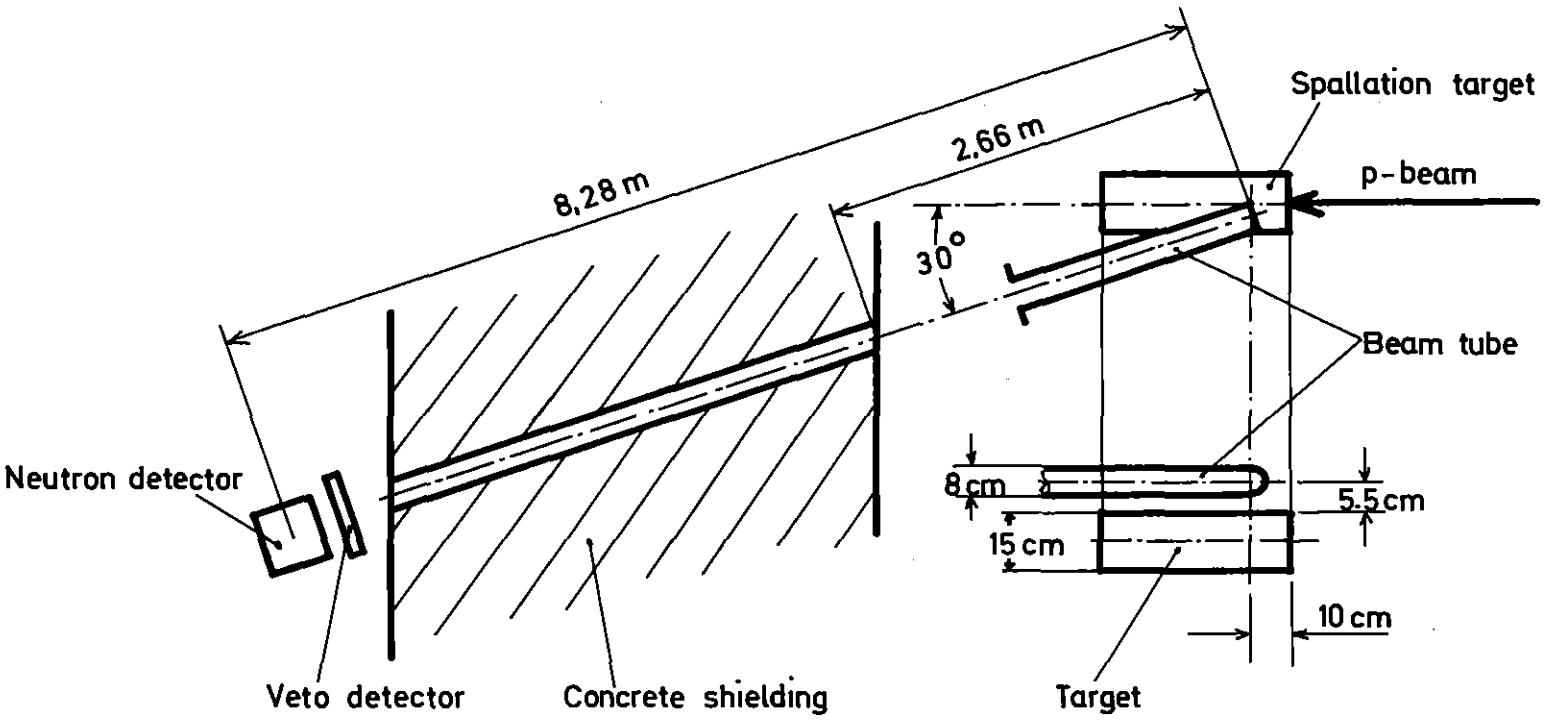

Figure 9 - Schematic diagram of the experimental arrangement used for the measurement of the fast neutron background accompanying the thermal beam

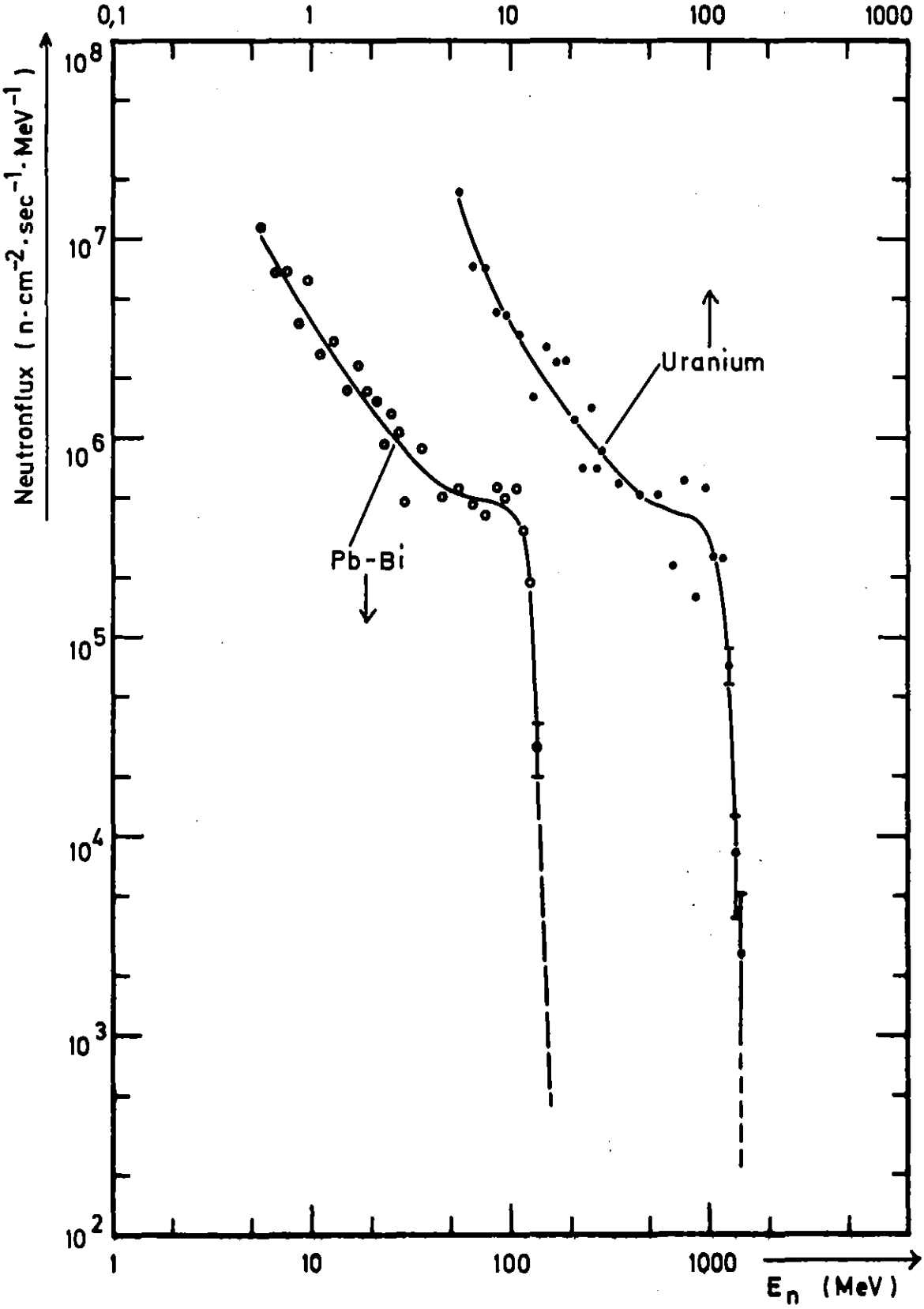

Figure 10 - Spectral distribution of fast neutrons in a light water moderated thermal neutron beam from 15 cm diam. Pb-Bi and U targets. Absolute neutron fluxes are given for a 10 mA proton current and a distance of 6 m from the target